IEEE Access
Multidisciplinary | Rapid Review | Open Access Journal

SPECIAL SECTION ON GREEN COMMUNICATIONS ON WIRELESS NETWORKS

Received April 7, 2019, accepted May 29, 2019, date of publication June 5, 2019, date of current version June 24, 2019.

Digital Object Identifier 10.1109/ACCESS.2019.2920924

Toward Energy Efficiency Aware Renewable Energy Management in Green Cellular Networks With Joint Coordination

ABU JAHID[1], (Student Member, IEEE), MD. SHAMIMUL ISLAM[2], MD. SANWAR HOSSAIN[1], MD. EMRAN HOSSAIN[3], MD. KAMRUL HASAN MONJU[3], AND MD. FARHAD HOSSAIN[4], (Member, IEEE)

[1]Department of Electrical, Electronic and Communication Engineering, Military Institute of Science and Technology, Dhaka 1216, Bangladesh
[2]Department of Electrical and Electronic Engineering, University of Information Technology and Sciences, Dhaka 1212, Bangladesh
[3]Department of Electrical and Electronic Engineering, Bangladesh University of Business and Technology, Dhaka 1216, Bangladesh
[4]Department of Electrical and Electronic Engineering, Bangladesh University of Engineering and Technology, Dhaka 1205, Bangladesh

Corresponding author: Abu Jahid (setujahid@gmail.com)

ABSTRACT In this paper, we focus on an essential energy management approach for enhancing energy efficiency (EE) as well as reducing fuel consumption of off-grid cellular networks whose base stations (BSs) are supplied with hybrid power sources including solar PV array and diesel generator (DG). To take the full advantage of PV technology, this paper examines the reliability performance and carbon footprint implications in addition to EE. This paper also investigates the benefits of unevenly harvested green energy sharing mechanism under zero fuel consumption scheme via physically installed resistive power lines taking into account of dynamic nature of renewable energy (RE) generation and traffic arrival density. Furthermore, joint transmission coordinated multipoint (JT-CoMP) user association technique is integrated for achieving higher throughput and EE performance providing the best SINR quality to a connected user equipment (UE). A comprehensive Monte-Carlo based simulation study has been carried out for evaluating EE, EE index (EEI), and energy saving performances in downlink LTE-advanced networks under a wide range of network settings. The results reveal that the proposed system can attain up to 26% energy savings via cooperation mechanism and 48.7% more energy efficient in terms of EEI under peak load over the conventional hybrid paradigm.

INDEX TERMS Renewable energy management, Green cellular network, Energy efficiency, Joint coordination, LTE-A.

I. INTRODUCTION

The widespread availability of affordable data-hungry devices and their diverse type of applications such as video streaming, cloud storage, social networking, multimedia services, etc. upsurge the data traffic demand enormously in wireless networks. A recent study carried out by Cisco reveals that the volume of data transmission between mobile device to device has increased by 69%, which is about 2.5 exabytes monthly. This study also emphasized that the ever-expanding mobile traffic will not likely to saturated for the next half of a decade instead it will continue to grow around tenfold [1]–[3]. Researchers anticipate that the mobile phone will be the main communication device especially in the rural areas that enables people to communicate which results a vast number of mobile phone subscriptions [4]. To handle the staggering wireless traffic evolution, cellular operators need to deploy an increased number of radio access network (RAN) and core infrastructure to support internet access everywhere providing the high bandwidth capacity. Consequently, this could lead massive electricity consumption and constitute higher capital and operational expenditures i.e. CAPEX and OPEX respectively accompanied by pollution intensive greenhouse gas (GHG) emissions.

Among all the other participants in the area of Information and Communication Technology (ICT), the BS avidly drains electricity around 60 to 80 percent of the total energy needed for the entire communication network and telecom operators are thereby facing exhaustive OPEX due to the power supply [5], [6]. The utilization of conventional energies like fossil fuels, coals increased carbon footprints caused by the operating cellular infrastructure. In the ICT sectors,

The associate editor coordinating the review of this manuscript and approving it for publication was Carol Fung.

telecommunication industries are responsible for contributing the maximum amount of pernicious gases to the atmosphere and the total carbon emissions is about 3-4% around the globe [7]. It is evident from the research that yearly power depletion around the world by the telecommunication sector has expanded from 219 TWh in 2007 to 354 TWh in 2012 with an annual growth rate of 10% [8]. Owing to the enormous pace of network expansion, the telecom sector over the planet will consume 51% of global energy in 2030 results a huge amount of greenhouse gas (GHG) secretions and higher operational expenditure (OPEX) [9]. It is expected that the global CO_2 emissions will rise by 20% within 2030 if cellular industries continue to use the conventional sources together with the utility bills [10]. In this regard, energy efficiency (EE) is the paramount consideration in order to reduce the net present cost and greenhouse gas (GHG) emissions with a greater degree of reliability and quality of service (QoS) in the context of green cellular networks [11].

Intending to solve the problems in the aforementioned paragraphs, several efforts are devoted to find energy efficient solutions with the intention of reducing cost, environment friendly and improving sustainability [12], [13]. The approach of renewable energy harvesting (REH) technology to power cellular base stations (BSs) is becoming a compelling solution to make them more independent from the conventional power supply [14], [15]. By considering these, network operators, academia and vendors are increasingly interested to deploy local RE generators for wireless data transmission which can radically reduce the grid energy depletion and improve network EE [16]–[18]. Renewable energy sources such as solar and wind has several advantages, for example, they are bountiful & omnipresent in the environment, cheap and toxic free. The fundamental challenges of utilizing green energy for BSs is the highly intermittent and random behavior of RE generation over time and space, resulting in a mismatch between the power supply and load demands. Therefore, standalone RE sources is not an extent efficient option to ensure zero outage of wireless communication owing to the tempo-spatial dynamics. Nowadays, one approach to tackle the challenges of variability of RE availability is adopting hybrid power supply solution, for example, PV/grid, WT/PV/DG or any other possible combination with sufficient energy storage capacity in order to improve the energy efficiency, system reliability and make the atmosphere greener as well [19].

Recently communication service providers also depend on diesel generator (DG) to provide electricity to the BS because of limited availability of grid supply or the utility grid is not available at all in some remote regions of the world. However, RE in conjunction with DG supply offers an attractive solution in terms of reliability and cost effectiveness in some rural areas where the connection of electricity grid is more expensive. Due to the several unfavorable factors like limited reserves of fossil fuel, global warming, acid rain and huge operational expenditure (OPEX), the conventional approach for instance grid electricity or DG can never be a viable option since they are not environmental friendly [20], [21]. The high CAPEX of a PV system is counterbalanced by the low capital cost of DG set, whereas the high OPEX is balanced by RE generators. In accordance with the trend, green cellular networking has drawn intensive attention among researchers concentrating on maximum utilization of solar energy in addition to the minimum fuel consumption. As a promising solution, combined PV/DG power supply has provided a greater level of reliability to counterbalance the temporal dynamics of RE generation aiming to ensure zero outage.

Various relevant recent work provisioning BS to be powered by hybrid supplies for improving EE in wireless cellular communication has been widely discussed in [21]–[25]. Reference [21] investigated the energy yield analysis including OPEX savings for the cellular BSs powered by aggregate PV/DG technology using HOMER software in Malaysia. Han and Ansari [22] proposed an optimization algorithm for minimizing on-grid energy consumption enabling more users to be served using solar energy in hybrid powered cellular BSs. Wang *et. al.* [23] proposed an user association algorithm based on the level of green energy availability in heterogenous cellular networks. Authors in [24] investigate the long-term feasibility of a combined solar-wind solution to cellular BSs targeting to the minimum net present cost. None of the manuscripts considered the variation of bandwidth, tempo-spatial traffic diversity, and energy efficiency calculation for different system setup. Renewable energy management paradigm refers to the maximum usage of energy harvesting facilities in the cellular BS that have common EE and environmental goals.

The amount of solar power generation is may be higher or lower in accordance with tempo-spatial traffic diversity and solar radiation intensity which often causes a mismatch with the BS load consumption. The concept of sharing surplus electricity among neighboring BSs via smart grid or external physical transmission lines has been recognized as an emerging solution in some literature [26]–[28]. An efficient energy cooperation framework among collocated BSs via smart grid based on the level of a priori knowledge about RE generation has been proposed in [28]. The potential benefits of energy cooperation mechanism on overall associated cost with hybrid supplies are thoroughly examined in consideration of temporal fluctuation of data arrivals in reference [29]. The realization of energy cooperation between two BSs over the externally connected power cables is discussed in [30]. The manuscripts do not investigate EE performance and the presence of traffic variation including carbon emission analysis. It is worth mention that energy sharing approach is not feasible for a sparse network with longer inter-site distance because of higher CAPEX, high transmission loss and a proper way of clearance for the transmission cables. Nevertheless, power sharing is plausible if locally available RE generation is high enough to serve its demand and then transfer excess electricity to the commercial grid or requesting BS. A combination of energy storage

and power sharing facility enables to balance the mismatch between the electricity generation and BS load demand in an energy efficient way.

Substantial research works have been carried out to optimizing the operation of green powered cellular infrastructures such as enhancement of throughput performance [31], reduction of greenhouse gas emissions [32], distributed RE generation [28] and centralized RE management [33] under the smart grid environment. But some of the models do not account any storage technology or coordination technique which incurs EE performance degradation in conventional grid system. Authors in [34] proposed on/off mechanism of small base stations according to the traffic demand with hybrid supplies for further improving EE performance. Sleep mode provision may deteriorates QoS due to lack of proper coordination technique. The uplink spectral efficiency of green cellular networks with JT CoMP technique is critically investigated in [35] without focusing on EE.

Conventional designs of mobile wireless networks primarily focused on spectral efficiency without any provision of EE. In addition, cellular operators have dimensioned their infrastructure based on peak load, thus over sizing system components restricts the efficient energy utilization during low traffic hours or empty arrivals. Unlike the above techniques, we adopted SINR based joint coordination user association technique to investigate the EE performances taking into considerations of some limiting factors under a wide range of setup. Being inspired from the aforementioned discussion and research gaps, this paper broadly explores the inherent benefits of renewable energy and joint BS coordination technique on energy efficiency and energy savings for off-grid LTE-A macrocell BS with Remote Radio Head (RRH) unit. Macro BS with RRH predominantly minimizes the feeder cable loss as the fiber optic link replaces the coaxial cable connection. Moreover, no cooling arrangement is required for RRH enabled BS and therefore, it contributes higher EE with a greater level of flexibility and desired quality of service (QoS). The prominent contributions of this paper are summarized as follows:

- A generalized hybrid PV/DG power supply is developed for the off-grid LTE-A cellular networks addressing reliability and ecological issues. Under the suggested framework, solar PV array plays as a primary energy source while the DG supply remains standby one. However, storage autonomy hours is also measured for reliability study in the case of both PV and DG failure simultaneously. In particular, we give prominence to energy savings through solar energy sharing policy based on surplus electricity production under low BS consumption.
- SINR-SINR based JT CoMP transmission technique is adopted for further improving EE in consideration of some limiting parameters such as inter-cell interference, shadow fading, and variability of load dependent BS power consumption.
- We examine the system performances in terms of energy yield, autonomy hours, EE and EEI varying system bandwidth, battery depth of discharge, load factor, etc. In addition, we figure out on-site PV panel capacity as well as excess electricity under different load factor and zero fuel consumption (ZFC) condition. Finally, the effectiveness of the proposed system is investigated comparing with the traditional hybrid scheme.

The rest of the paper is organized as follows. The system model including BS power consumption scenario, solar energy generation model, energy storage system, and DG system are discussed in section II. Section III outlined the detailed performance analysis. Simulation setup, comparison analysis, environmental aspect, and energy yield evaluation are also discussed extensively with insightful comments in this section. Finally, the conclusion has drawn in section IV.

II. SYSTEM MODEL

This section presents the system model along with joint transmission CoMP technique, energy sharing framework, wireless link model and the formulation of performance metrics.

A. NETWORK ARCHITECTURE

A downlink LTE-A cellular networks having a set of N collocated BSs $\mathbb{B} = \{\mathcal{B}_1, \mathcal{B}_2, ..., \mathcal{B}_N\}$ and covering an area $\mathcal{A} = \{\mathcal{A}_1 \cup \mathcal{A}_2 \cup ... \cup \mathcal{A}_N\} \subset \mathbb{R}^2$ is considered. Here, $\mathcal{A}_i$ is the coverage area of BS $\mathcal{B}_i, \forall i \epsilon \{1, ..., N\}$. We assume the macro base stations are installed with tri-sector 2/2/2 arrangements in a hexagonal grid fashion with remote radio head (RRH) unit. Needless to say, a macro BS contains transceiver (TRX) unit, radio frequency (RF) unit, power amplifier (PA) sections, and a baseband (BB) unit for signal processing and coding. On the other hand, orthogonal frequency bands are allocated in a BS using OFDMA technique to cancel out intra-cell interference. Fig. 1 shows the network layout consisting of two subsystems, the telecommunication load and power supply unit. A JT CoMP technique is deployed for receiving best signal intensity to associated UEs.

The BSs in the considered cellular networks are powered with a set of solar photovoltaic (PV) cells and battery bank as an energy storage device. Besides, a diesel generator is kept as a complementary energy source to handle network outage during EH malfunctions. For sharing unevenly generated power, all BSs in the first tier are connected via resistive power cables for the envisaged green cellular framework. An electronic converter is connected between DC and AC bus for energy conversion according to the BS demand. Furthermore, an intelligent energy management unit (EMU) is installed for smart charge controlling to prevent the battery from over charging and over discharging.

B. JOINT TRANSMISSION COORDINATED MULTIPOINT (JT CoMP)

In coordinated multipoint (CoMP) technique, several BSs coordinate with each other such a way that it increases throughput by reducing inter-cell interference. In general,

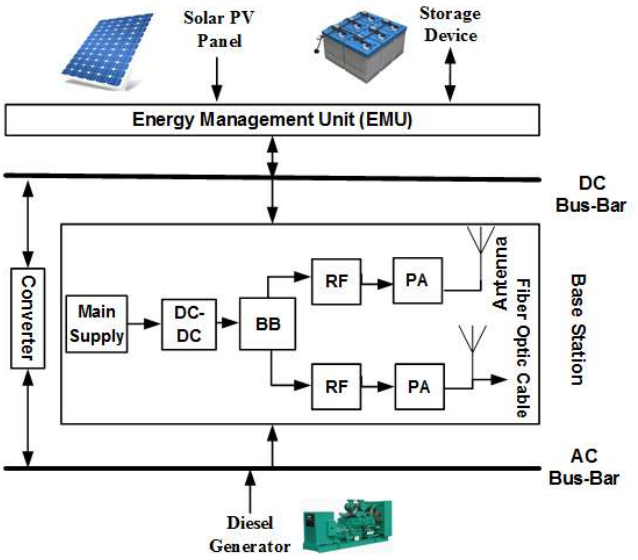

FIGURE 1. Proposed network model.

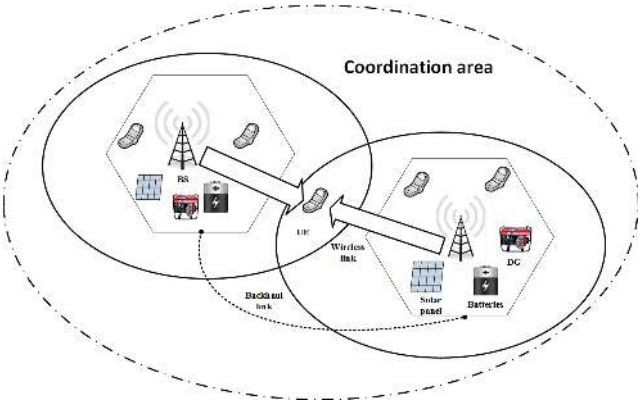

FIGURE 2. JT CoMP transmission technique.

a UE is typically connected with nearest BS regardless of the signal quality. The closest BS may not always support better signal strength due to fading and interference. Under JT CoMP transmission, data is transferred to a user equipment (UE) simultaneously from multiple coordinated BSs in order to strengthen received signal quality [36], [37]. A UE ranks the BSs in a descending manner based on received signal quality under the given cluster. In this paper, two BSs providing maximum SINR are selected for serving associated UEs jointly. Fig. 2 depicts the two selected BSs jointly serve a single UE for better throughput performance.

C. BS POWER MODEL

The power dissipation of a BS depends largely on the corresponding traffic arrival rate. The cellular network traffic volumes are hugely dynamic over time and space. Typically, a cellular network operator designed the energy infrastructure for BS considering the full load condition which results a huge amount of energy wastage during the ideal state.

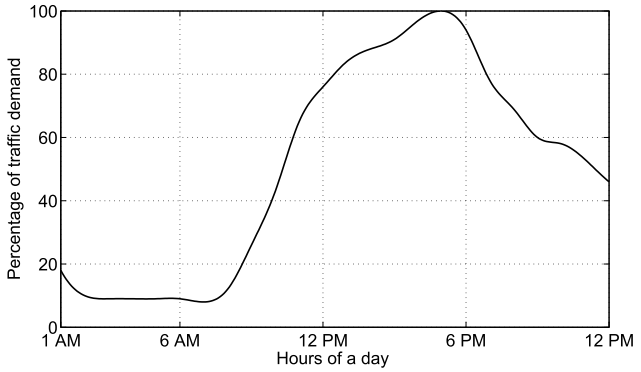

FIGURE 3. Daily traffic load profile.

Therefore, it is necessary to design the energy system for BS according to the real traffic load in order to avoid electricity wastage. The BS consumes electricity in two different ways: static power consumption and dynamic power consumption. The approximated daily traffic load profile is exhibited in Fig. 3 which can be evaluated by Poisson distribution model as follows

$$\lambda(t) = \frac{p(t,\alpha)}{max[p(t,\alpha)]} \tag{1}$$

$$p(t,\alpha) = \frac{\alpha^t}{t!}e^{-\alpha} \tag{2}$$

where $\lambda(t)$ is the normalized traffic distribution, $p(t,\alpha)$ is the Poisson distribution function of traffic demand at a particular period of time, and α is the mean value where peak number of traffic arrivals occur at 5 PM. The normalized traffic demand in a time slot establish the relationship between the number of active users and the number of resource blocks (RBs) to serve users. If the number active users is greater than the available resource blocks, a new incoming user cannot be served. UEs are considered to be uniformly distributed over the geographical area.

Let us assume the number of transceivers of a typical BS be (N_{TRX}) and actual traffic intensity is (χ), then the total estimated power dissipation for BS is defined as [38]

$$P_{in} = \begin{cases} N_{TRX}[P_1 + \triangle_p P_{TX}(\chi - 1)], & \text{if } 0 < \chi \leq 1 \\ N_{TRX}P_{slp}, & \text{if } \chi = 0 \end{cases} \tag{3}$$

$$N_{TRX} = N_{sec} \times N_{ant} \times N_{sc} \tag{4}$$

where N_{sec} and N_{ant} denotes the number of sectors and number of antennas per sector respectively. The notation N_{sc} presents the number of sub-carries to allocate RBs. $P_1 = P_0 + \triangle_p P_{TX}$ is the the maximum power consumption of a BS sector and P_0 is the consumption at idle state. P_{TX} is the BS transmission power typically 43 dBm (i.e. 20W). The load dependency is accounted for the power gradient, $\triangle_p$. The scaling parameter $\chi = 1$ indicates that a fully loaded system and $\chi = 0$ indicates idle state. Furthermore, a BS without any traffic load enters into sleep mode with lowered consumption, P_{slp}. The dynamic power

TABLE 1. BS approximate power consumption model parameters [8].

BS Type	N_{TRX}	$P_{TX}[W]$	$P_0[W]$	$\triangle_P$	$P_{slp}[W]$
Macro w/o RRH	6	20	130	4.7	75
Macro with RRH	6	20	84	2.8	56

consumption is varied with traffic loading parameter (χ). The parameters of BS load are summarized in Table 1. Now P_1 can be expressed as below [8]

$$P_1 = \frac{P_{BB} + P_{RF} + P_{PA}}{(1-\sigma_{DC})(1-\sigma_{MS})(1-\sigma_{cool})} \tag{5}$$

where P_{BB} and P_{RF} are the power consumption scaled linearly with the transmission bandwidth $\mathcal{BW}$ and the number of transceiver chain (N_{TRX}) and they can be evaluated as [8]

$$P_{BB} = N_{TRX}\frac{\mathcal{BW}}{10\ MHz}P'_{BB} \tag{6}$$

$$P_{RF} = N_{TRX}\frac{\mathcal{BW}}{10MHz}P'_{RF} \tag{7}$$

where P'_{BB} and P'_{RF} are the power consumption of baseband unit and radio frequency transceiver respectively. Losses incurred by DC-DC power supply, mains supply and active cooling can be approximated by the loss factors σ_{DC}, σ_{MS} and σ_{cool} respectively. However, power consumption in the power amplifiers is represented by P_{PA} which depends on the maximum transmission power and power amplifier efficiency η_{PA} and can be given as follows

$$P_{PA} = \frac{P_{TX}}{\eta_{PA}(1-\sigma_{fd})} \tag{8}$$

The power dissipation of the cooling unit hinges on the interior temperature of the BS cabinet and typically a macro BS absorbs roughly 10% of total energy without the facility of RRH [8]. However, no cooling equipment is required for macro BS with RRH. The total BS power consumption for the macro BS with RRH and without RRH is presented in Table 2 under peak traffic load showing the power expenditure of each individual element. RRH enabled macro BS has substantially reduced energy consumption (about 44% under 10 MHz transmission bandwidth) over conventional macrocell as observed from Table 2. As a consequence, the rest of the analysis will be carried out for macro BS with RRH configuration since it requires lower installed capacity with desired QoS. Another crucial parameter load factor (L_f) can be defined as the ratio of occupied resource block (RB_o) and the total available resource blocks (RB_t).

$$L_f = \frac{RB_o}{RB_t} \tag{9}$$

Fig. 4 shows the BS power consumption for different transmission bandwidth over a day. The dynamic BS power consumption is directly varied with traffic loading parameter χ as seen from Fig. 4. According to the definition, higher system bandwidth pushed BS power consumption in an upward direction. To handle cumbersome BS load demand, a large

TABLE 2. Macro BS power consumption at maximum load of a LTE system for 10 MHz bandwidth [8].

Components	Parameters	w/o RRH	with RRH
BS	Type	Macro	Macro
	P_{TX} [W]	20	20
	Feeder loss σ_{fd} [dB]	3	0
PA	Back-off [dB]	8	8
	Max PA out [dBm]	54	51
	PA efficiency η_{PA} [%]	31.1	31.1
	Total PA [W]	128.2	64.4
RF	P_{TX} [W]	6.8	6.8
	P_{RX} [W]	6.1	6.1
	Total RF, P'_{RF} [W]	12.9	12.9
Baseband, BB	Radio (inner Tx/Rx)[W]	10.8	10.8
	Turbo (outer Tx/Rx)[W]	8.8	8.8
	Processors [W]	10	10
	Total BB, P'_{BB} [W]	29.6	29.6
DC-DC	σ_{DC} [%]	7.5	7.5
Cooling	σ_{cool} [%]	10	0
Mains Supply	σ_{MS} [%]	9	9
Sectors		3	3
Antennas		2	2
Total power[W]		**1350**	**754.8**

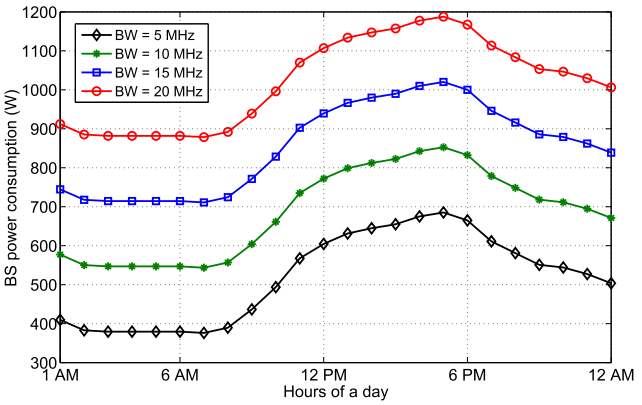

FIGURE 4. Daily BS power consumption for various *BW*.

number of solar modules and battery bank need to be installed to support massive traffic arrivals under higher bandwidth.

D. WIRELESS LINK MODEL

We consider log-normally distributed shadow fading as a propagation channel model to derive signal to interference plus noise ratio (SINR). If d is the distance between BS (i.e. transmitter) and a UE (i.e. receiver), then the path loss in dB can be expressed as

$$PL(d) = PL(d_0) + 10\zeta log(\frac{d}{d_0}) + X_\sigma \tag{10}$$

where $PL(d_0)$ is the path loss in dB at a reference distance d_0 and ζ is the path loss exponent. $PL(d_0)$ can be calculated

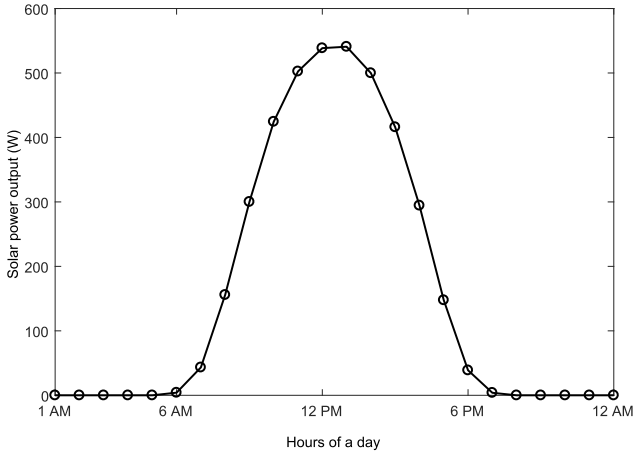

FIGURE 5. PV power output over a day.

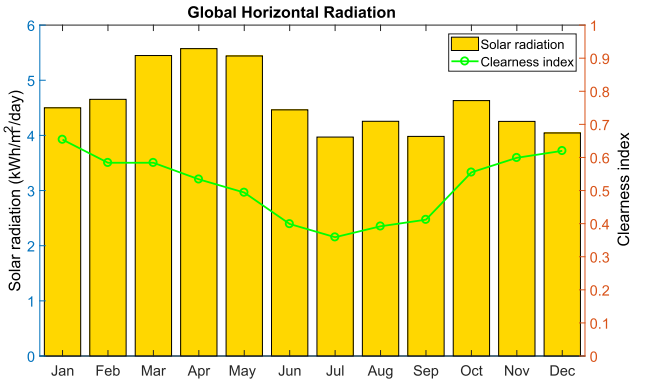

FIGURE 6. Average annual profile of solar radiation in Bangladesh.

using the free-space path loss equation. X_σ is the amount of shadow fading modeled as a zero-mean Gaussian random variable with a standard deviation σ dB.

Thus, the received power in dBm for k^{th} UE from i^{th} BS $\mathcal{B}_i$ is given by

$$P_{rx}^{i,k} = P_{tx}^{i,k} - PL(d) \tag{11}$$

where $P_{tx}^{i,k}$ is the transmitted power in dBm. The transmit power $P_{tx}^{i,k}$ from B_i to UE k satisfies $\sum_{k\epsilon U} P_{tx}^{i,k} \leq P_i^{max}$, where P_i^{max} is RF output power of BS $\mathcal{B}_i$ at its maximum traffic load. However, two coordinated BSs jointly serve a single UE under JT CoMP transmission technique. Therefore, the received power at CoMP-UE can be expressed as

$$P'_{rx} = P_{tx}^{1,k} + P_{tx}^{2,k} - PL(d) + X_\sigma \tag{12}$$

where $P_{tx}^{1,k}$ and $P_{tx}^{2,k}$ is the transmitted power in dBm from selected two coordinated active BSs respectively. On the other hand, the inter-cell interference ($\mathcal{P}_{k,inter}$) can be expressed as:

$$\mathcal{P}_{k,inter} = P_{inter}^{i,k} = \sum_{m\neq 1,2} (P_{tx}^{m,k}) \tag{13}$$

Then the received SINR $\gamma_{i,k}$ at k^{th} UE from BS $\mathcal{B}_i$ can be given by

$$\gamma_{i,k} = \frac{P_{rx}^{i,k}}{\mathcal{P}_{k,inter} + \mathcal{P}_{k,intra} + \mathcal{P}_N} \tag{14}$$

where $\mathcal{P}_{k,intra}$ is the intra-cell interference, $\mathcal{P}_N$ is the additive white Gaussian noise (AWGN) power given by $\mathcal{P}_N = -174 + 10log_{10}(\mathcal{BW})$ in dBm and $\mathcal{BW}$ is the transmission bandwidth in Hz. In this paper, the proposed network model is simulated considering inter-cell interference from neighboring macrocells as interferes in a regularly spaced hexagonal deployment scenario.

E. PHOTOVOLTAIC (PV) ARRAY

The sunlight is ubiquitous and contamination free ambient source on this planet. Solar PV modules are placed together in series/parallel to form the solar array which converts solar irradiation into DC electrical energy. The solar power generation mainly relies on some factors such as terrestrial region, materials of panel, environmental consequences, tracking mode and panels tilt. The solar panel generates power in an intermittent manner all over the day and it follows a normal distribution pattern. Fig. 5 shows the temporal diversity of solar power output for 1 kW PV module which is estimated using System Advisory Model (SAM) without any tracking mode for Patenga area in Bangladesh [36]. Fig. 6 represents the average yearly solar radiation profile with a clearness index for Patenga.

The RE generated at BS $i \epsilon$ {1,...,N} during time slot n is a random variable denoted by $r_i\ (t) \epsilon\ [0, r_i{}^{max}]$, where $r_i{}^{max}$ is maximum available solar energy generation by $\mathcal{B}_i$. The green power generation can be defined as $\int_{(n-1)\tau}^{n\tau} b_i(t)dt = r_i(t)$, where $b_i(t)$ is obtained from the instantaneous solar power profile as depict in Fig. 2 and τ is the duration of each time slot.

The time varying average solar energy generation, $\bar{r}_i(t)$ is characterized by the following model [28]:

$$\bar{r}_i(t) = \frac{r_i{}^{max} exp^{-(n-\beta_i)^2}}{\delta_i^2}\tau \tag{15}$$

In this model, the parameter β_i represents the position in time of the peak generation, chosen to be noon, i.e. 12 hours, $\forall i\epsilon\{1, ..., N\}$, δ_i indicates the shape width at half maximum of the peak, chosen to be 3 hours, $\forall i\epsilon\{1, ..., N\}$, and the time duration of each slot τ is one hour. On the other hand, the annual solar energy generation can be given by the following formula [8]

$$E_{sol} = C_{sol} \times \Delta_r \times F_d \times \delta \times 365\ days/yr \tag{16}$$

where C_{sol} the rated solar PV (SPV) array capacity in kW, Δ_r is the average daily solar radiation intensity in $kWh/m^2/day$ (4.59 as seen from Fig. 6), δ is the dual axis tracking factor (usually 1.3), and F_d is the derating factor accounts the effects of dust, wire loss, temperature fluctuations etc. on the SPV energy production.

TABLE 3. Solar panel specifications.

Specifications	Type (Value)
Solar module type	Sharp ND-250QC (poly crystalline)
Generation technology	CSP PV cell
Nominal voltage (V)	29.80 VDC
Nominal current (A)	8.40 Amp
Maximum power (P_{max})	250 Watt
Open circuit voltage (V_{oc})	38.3 VDC
Short circuit current (I_{sc})	8.90 Amp
Tracking mode	Dual axis

The parameters of solar module used in this paper are summarized in the Table 3.

F. DIESEL GENERATOR

Since the solar energy is unable to feed the BS demand independently, hence DG supply could mitigate the fluctuations of RE generation and enhance the battery lifetime. SPV/DG hybrid system is considered as a more viable solution over standalone DG or SPV power supply system due to the compensating relation between SPV and DG. The electrical energy generation by a DG (E_{DG}) can be expressed as

$$E_{DG} = P_{DG} \times \eta_{DG} \times t_r, \quad kWh \tag{17}$$

where P_{DG} the rated power output, η_{DG} is the DG efficiency and t_r is the DG running duration. Fuel consumption can be calculated as

$$F_C = E_{DG} \times F_{sp} \tag{18}$$

where F_{sp} is the specific fuel consumption (L/kWh).

G. ENERGY STORAGE SYSTEM (ESS)

Several batteries are interconnected in series/parallel in order to build the energy storage unit which is used to supply the BS during the insufficient solar generation, sudden increment of load demand and natural disturbance etc. The storage unit consumes the excess electricity and discharge when the solar PV array or DG sources are unable to feed the BS load and thereby improves the system reliability without interruption [38]. Typically, lead-acid batteries (Trojon L16P) are widely used in the cellular BSs due to low weight, modular, high energy density and high storage efficiency [36], [38]. Battery depth of discharge (B_{DOD}) illustrates how deeply the battery is discharged, complement to the state of charge (B_{SOC}). For instance, $B_{DOD} = 80\%$ means the battery has delivered 80% of its energy, whereas 20% energy will be reserved. Alternately, 20% reserves energy identifies the battery SOC. However, B_{DOD} can be expressed as follows

$$B_{DOD} = (1 - \frac{B_{SOC_{min}}}{100}) \tag{19}$$

where $B_{SOC_{min}}$ is the minimum SOC of battery denotes the lower threshold limit of battery discharge.

The battery bank capacity (B_c) determines the backup time for solar PV array, can be expressed as [38]

$$B_c = \frac{P_{BS} \times D \times t_w}{B_{DOD} \times V_b \times K_b} \quad Ah \tag{20}$$

where P_{BS} is the BS DC power load, D is the backup days, K_b is the coefficient of battery capacity (=1.14), t_w is the working time in a day, and V_b is the battery voltage operated at 48 V DC bus-bar.

The maximum and minimum battery bank storage capacity in kWh can be determined as follows

$$E_{battmax} = \frac{N_{bat} \times V_{nom} \times Q_{nom}}{1000} \times B_{SOC\,max} \tag{21}$$

$$E_{battmin} = \frac{N_{bat} \times V_{nom} \times Q_{nom}}{1000} \times B_{SOC\,min} \tag{22}$$

Note that ESS capacity should not exceed the maximum limit and not reached the below threshold level. The available battery bank capacity at every hour t can be estimated as follows

$$E_{batt}(t) = \lambda \times E_{batt}(t-1) + E_{in}(t) \times \eta_C - E_{BS}(t) \tag{23}$$

$$E_{in}(t) = E_{DC} + E_{AC} = E_{sol} + E_{DG} \tag{24}$$

where $E_{batt}(t-1)$ is the energy storage capacity in previous hour, $E_{in}(t)$ is the incoming energy from both DC and AC power sources such as solar PV modules and fuel generator. λ is the charging efficiency of battery i.e., the percentage of storage energy retained after a unit period of time and (1-λ) indicates the storage deficiency factor. For example, $\lambda = 0.9$ indicates that 90% stored energy is useful while 10% energy will be lost in the storage during the time interval. $E_{BS}(t)$ represents the hourly energy demand by the LTE cellular BS and η_C represents the conversion efficiency. The initialization condition for the batteries is $E_{in}(0) = 0, \forall i \epsilon \{1, ..., N\}$.

The size of battery bank depends on the BS power consumption and the duration that support BS load demand independently. The larger battery bank capacity takes a longer time to take charge and leading to high operating cost.

Battery bank autonomy (B_{aut}) defines the number of hours that support BS load without any help from an external retailer. This parameter plays a significant role during hybrid supply malfunctions and signifies the reliability performance with zero energy shortage. B_{aut} can be defined as follows [38]

$$B_{aut} = \frac{N_{bat} \times V_{nom} \times Q_{nom} \times B_{DOD} \times (24h/day)}{L_{BS}} \tag{25}$$

where L_{BS} average daily BS load in kWh, N_{bat} is the number of battery cells in the battery bank, V_{nom} is the nominal voltage of each battery cell (V) and Q_{nom} is the nominal capacity of single battery in Ah. Table 4 shows the nominal battery capacity and voltage for the two different ESS. Owing to the high power output, type-1 lead-acid battery bank is considered throughout this paper.

TABLE 4. Energy storage specifications.

Parameters	Type-1	Type-2
Nominal voltage (V_{nom})	6 VDC	12 VDC
Nominal capacity (Q_{nom})	360 Ah	120 Ah

H. ENERGY SHARING STRATEGY

Two way energy trading allows better utilization of green energy from the surplus power generation. Energy cooperation among collocated BSs may take places on different energy availability which directly depends on traffic load dependent BS power profile and tempo-spatial variation of RE generation. Under the proposed model, surplus electricity (E_{sur}) is produced when the supply energy exceeds the BS energy expenditure including battery loss (B_l) and converter loss (C_l).

$$E_{sur} = E_{in} - E_{BS} - B_l - C_l \tag{26}$$

In this paper, we assume B_l and C_l comprises with 10% and 5% of the total power consumption respectively. By combining the supply and demand sides, $E_{sur} > 0$ shows the excess energy generation status and $E_{sur} < 0$ indicates the deficit status of i^{th} BS. Since energy sharing is too complex for a large number of BSs and longer inter-site distance. In this paper, we assume energy sharing take place only first cellular tier consisting of seven BSs via shortest connecting path. However, sharing power between two BSs will result line losses due to resistive heating. The net energy shared (E_{sh}) between neighboring BSs can be computed as

$$E_{sh}(t) = E_{sur}(t) - E_l(t) \tag{27}$$

where $E_l(t)$ is the energy loss in the resistive conductor in the form of heat during energy trading. $E_l(t)$ is a function of connected conductor length and can be evaluated over t_o duration in hours as follows:

$$E_l(t) = I^2 R(l) \times t_o = \frac{P_{sh}^2 \times \rho \frac{l}{A_c}}{V^2} \times t_o \tag{28}$$

where I is the current traveling through the transmission line, $R(l)$ is the resistance of the l km conductor length, ρ in ohm-m presents the resistivity of the overhead line, A_c represents the cross-sectional area of the conductor in m^2, V is the DC bus-bar voltage (BS operated at 48 V DC). We assume the surplus energy cooperation take place in the DC form over the small geographical region.

The average energy savings via energy cooperation can be formulated as

$$AES(i,t) = \frac{\sum_{i=1}^{N} E_{sh}(t)}{\sum_{i=1}^{N} E_{BS}(t)} \times 100\% \tag{29}$$

where N is the number of transmitting BS, typically 7 BSs for the single-tier configuration.

Note that the resistance of the power cable is 3.276 ohm/km as obtained from the American Wire Gauge (AWG) conductor size standard [39]. The inter-site distance (ISD) is calculated as $\sqrt{3}$ times of cell radius (i.e. $\sqrt{3}R$).

However, the energy cooperation option is more feasible where the commercial grid supply is not present especially in remote areas which enhances EE performance by reducing fuel consumption. For power sharing, the particular BS ranks its surrounded BSs in a descending order based on available solar energy storage. Under the proposed model, the green energy utilization, fuel consumption and energy sharing phenomenon of i^{th} BS can be expressed as follows

CASE I: $E_{SOL} > E_{BS}$

i^{th} BS has sufficient solar energy for serving its associated users. Thus, there is no need of diesel consumption and energy sharing. The remaining harvested energy is stored in the battery bank after fulfilling its own demand which can be expressed as

$$E_{batt}(t) = E_{sol}(t) - E_{BS}(t) \tag{30}$$

Therefore, after satisfying the demand of time t, available energy in the storage of $\mathcal{B}_i$ for the time slot $(t+1)$ can be written as

$$E_{batt}(t+1) = \lambda \times E_{batt}(t) + E_{sol}(t+1) - E_{BS}(t+1) \tag{31}$$

CASE II: $E_{SOL} < E_{BS}$

When the solar energy production is less than BS demand, the $\mathcal{BS}_i$ seeks additional energy from its neighbors, which is the total energy remaining in their own storage. Hence, the total solar energy required to be shared by $\mathcal{B}_i$ at time t can be expressed as

$$E_{req}(t) = E_{BS}(t) - E_{sol}(t) \tag{32}$$

Consider the set of sorted BSs in a descending fashion is given by $\{\mathcal{B}_{i,1}, \mathcal{B}_{i,2}, ..., \mathcal{B}_{i,M}\}$, where M is the number of neighboring BSs of $\mathcal{B}_i$. Now, if the first neighboring BS $\mathcal{B}_{i,1}$ has required solar energy $\geq E_{req}(t)$, BS $\mathcal{B}_i$ fulfills its demand from $\mathcal{B}^{i,1}$. If the shared energy of $\mathcal{B}^{i,1}$ is not sufficient (i.e., $< E_{req}(t)$), BS $\mathcal{B}_i$ accepts the amount from $\mathcal{B}^{i,1}$ that it can share. Besides, it continues to seek additional energy from next BS from the given set for the remaining amount of required energy. Let $\mathcal{E}_{sh}^{i,m}$ be the amount of solar energy shared by $\mathcal{B}_i$ from the neighboring BS $\mathcal{B}_{i,m}$. Then the total energy received by $\mathcal{B}_i$ from the neighboring BSs can be given by

$$\mathbb{E}_i = \sum_{m=1}^{M} \mathcal{E}_{sh}^{i,m} \tag{33}$$

CASE III: $E_{SOL} + E_{sh} < E_{BS}$

When the combined solar energy and shared energy is less than BS demand, then DG supply is required to mitigate the shortage energy demand. Thus, the DG energy consumption, $E'_{DG}(t)$ by i^{th} BS is now

$$E'_{DG}(t) = E_{BS}(t) - E_{sol}(t) - E_{sh}(t) \tag{34}$$

In other words, the fuel generator is used to offset the remaining energy consumption whenever the allocated green energy is insufficient.

I. ENERGY EFFICIENCY METRICS

To examine the performance of green wireless network, it is necessary to evaluate the energy efficiency (EE) metrics in terms of bit per joule which defines as the ratio of data transmission rate to the level of power requirement. In this article, we consider the EE metric is the ratio between total throughput of the proposed framework and the net power (P_{net}) consumption of diesel generator. According to the Shanon Hartley's information capacity theorem, the total achievable throughput in a network at time t can be expressed by

$$T_{total}(t) = \sum_{k=1}^{U}\sum_{i=1}^{N} \mathcal{BW} log_2(1+\gamma_{i,k}) \quad bps \tag{35}$$

where N is the number of transmitting BSs and U is the total number of UEs in the network. Thus, the EE metric denoted as η_{EE} for time t can be written as

$$\eta_{EE}(t) = \frac{T_{total}(t)}{P_{DG}(t)} \quad bits/joule \tag{36}$$

where $P_{DG}(t) = \sum_{i=1}^{N} P_{in}(i,t) - \sum_{i=1}^{N} P_s(i,t)$ is the net energy consumption from the diesel generator in all the BSs at time t, $P_{in}(t)$ is the necessitated total power in BS $\mathcal{B}_i$ at time t and $P_s(t)$ is the green power from the solar source consumed by the BS $\mathcal{B}_i$ at time t.

Another important metrics called the energy efficiency index (EEI) is introduced in this manuscript to justify the CoMP effect on the proposed scheme. EEI can be defined as the ratio of total achievable throughput and BS input power consumption.

III. PERFORMANCE ANALYSIS

This section evaluates the performance of the proposed network powered by solar PV and DG supplies with sufficient storage capacity varying different system parameters such as load factor, bandwidth, battery depth of discharge, etc. Energy yield analysis and carbon footprint are also discussed in the same section.

A. SIMULATION SETUP

A MATLAB based Monte-Carlo simulation is carried out in where each data point are calculated by averaging 10000 independent iterations. Without loss of generality, we will consider one resource block (RB) is occupied by a single active UE. We assume the same BS power profile parameters for all the BSs, while equal transmit power is considered for all RBs. Inter-cell interference contributions by the neighboring BSs surrounded in a single tier are taken into consideration for the presented results. The spatial variability of traffic distribution among BSs is modeled as a uniform random variable in [0 1]. A summary of the system parameters of the simulated network considered in reference to the LTE standards [36] is presented in Table 5.

TABLE 5. Simulation parameters.

Parameters	Value
Resource block (RB) bandwidth	180 kHz
System bandwidth, $\mathcal{BW}$	5, 10, 15, 20 MHz (25, 50, 75, 100 RBs)
Carrier frequency, f_c	2.1 GHz
Duplex Mode	FDD
Cell radius	1000 m
BS Transmission Power	43 dBm
Noise power density	-174 dBm/Hz
Number of sectors	3
Number of antennas	2
Number of carriers	1
Reference distance, d_0	100m
Path loss exponent, n	3.574
Shadow fading, σ	8 dB
Access technique, DL	OFDMA
Traffic model	Randomly distributed

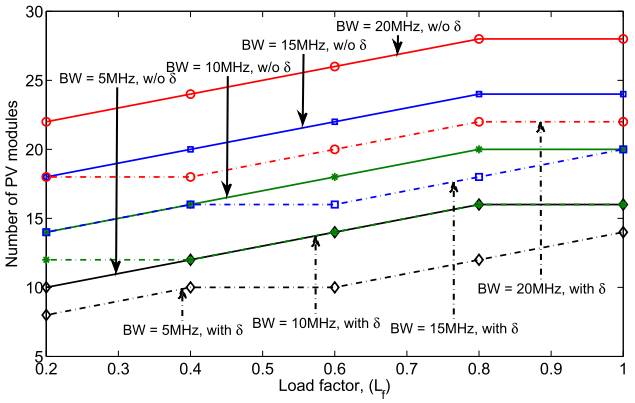

FIGURE 7. Number of PV modules vs L_f for different $\mathcal{BW}$ with δ and without δ.

B. RESULT ANALYSIS

We emphasize on EH capacity, installed storage capacity, excess electricity, energy savings via sharing, throughput, EE, and EEI performances including carbon emissions analysis to justify the effectiveness of the proposed system.

1) SYSTEM LAYOUT

Fig. 7 shows the required number of PV modules (N_{PV}) with load factor (L_f) varying system bandwidth illustrating the impact of dual axis tracking mode factor δ. The solid line presents the solar system without dual axis tracking factor and the dotted line indicates the system demands EH capacity with δ. The tracking method enables the PV module to capture more sunlight thus, more power will produce from the same PV panels compared to the fixed solar cell implementation. Needless to say that solar PV array with δ constitutes high capital cost but installing a movable solar panel is a more suitable option in terms of

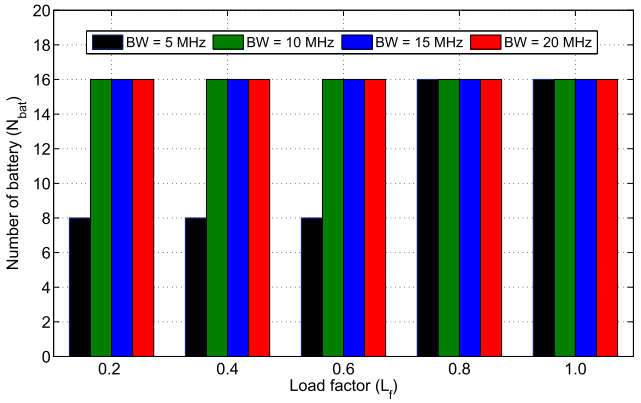

FIGURE 8. Number of batteries vs L_f varying $\mathcal{BW}$.

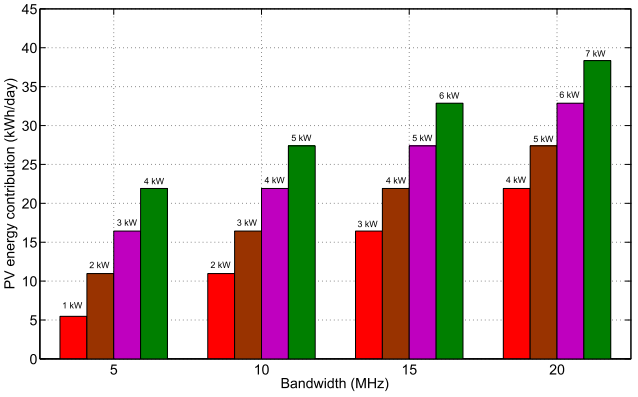

FIGURE 9. PV energy contribution vs $\mathcal{BW}$ varying PV capacity.

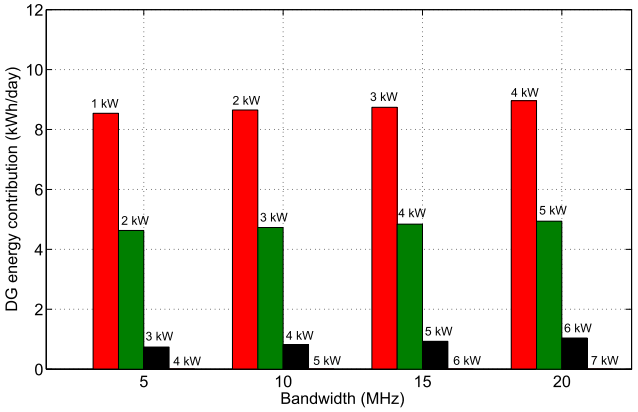

FIGURE 10. DG energy contribution vs $\mathcal{BW}$ varying PV capacity.

higher power generation as it involves the same operational expenses with that of non-tracking PV array over the 25 years lifetime of Sharp polycrystalline module. This mechanism significantly reduces the number of PV module as clearly evident in the Fig. 7. For example, the number of Sharp ND-250QC PV panels are needed of 12 and 16 with δ and without δ respectively for 50% load factor under 10 MHz $\mathcal{BW}$. The number of required PV panels increases linearly with the system bandwidth regardless of the tracking mode condition. Moreover, higher L_f uplifts N_{PV} as seen from the depicted figure to support a healthy amount of power supply during peak traffic arrivals. As seen, the maximum number of required modules are 28 when the load factor is 1.0 under system bandwidth of 20MHz. However, the results presented in the next section will be derived for the solar array with dual axis mode technique. For the sake of simplicity, the cost analysis is not discussed in this paper.

Fig. 8 illustrates the requisite number of battery cells (N_{bat}) in a battery bank for different load factor (L_f) varying bandwidth. The number of battery cells is found higher for large $\mathcal{BW}$ and higher L_f as it is varies with N_{PV} capacity. It is observed that the number of batteries remains constant for all the system bandwidth for 80-100% load factor.

2) ENERGY YIELD EVALUATION

The yearly contribution of energy by the individual energy sources such as solar PV and DG, battery bank autonomy and surplus electricity is examined in this section based on system configuration.

a: SOLAR PV ARRAY

The annual energy contribution of 5 kW solar array for an average daily radiation can be computed using Eq. (16); 5 kW (C_{sol}) $\times$ 4.59 kWh/m^2/day (Δ_{avg}) $\times$ 0.9 (F_d) $=$ 20.66 kWh per day. A dual-axis tacker mechanism elevates the total amount of energy by 30% [38] to be 26.85 kWh.

b: DIESEL GENERATOR

According to Eq. (17), 1 kW DG generates maximum 9.6 kWh/day; (P_{DG} $=$ 1 kW $\times$ η_{DG} $=$ 40% $\times$ t_{op} $=$ 24 hr). Fuel consumption has a direct relationship with the DG operating hours and load demand of the BS. If the solar radiation or the solar capacity is higher, then the DG requires to produce less amount of energy. Additionally, the DG running hour accelerates for the higher bandwidth and any malfunction of PV array or the energy storage module. Furthermore, the system performance enhances for large solar irradiation or PV installed capacity in terms of diesel consumption and GHG emissions reduction. Notably, 1 kW DG is used throughout this paper and the variation of daily solar radiation intensity is excluded in this paper.

Solar energy contribution for different bandwidth and PV capacity is depicted in Fig. 9. It is apparent that the energy contribution moves upward with the increment of PV capacity in accordance with $\mathcal{BW}$. Fig. 10 presents the amount of energy taken from the DG set for different $\mathcal{BW}$ varying on-site solar capacity (C_{sol}). As expected, fuel consumption decreases significantly with the higher value of C_{sol} i.e. E_{DG} follows an opposite fashion of E_{sol}. On the other hand, DG energy contribution almost remains unchanged for different $\mathcal{BW}$ due to the linear variation of C_{sol}. The empty region

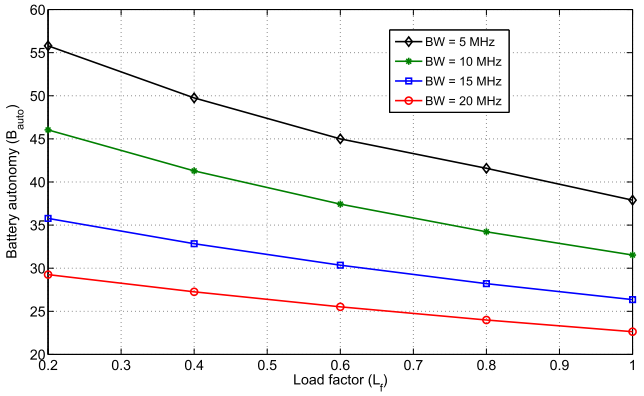

FIGURE 11. Battery autonomy vs load factor for different $\mathcal{BW}$.

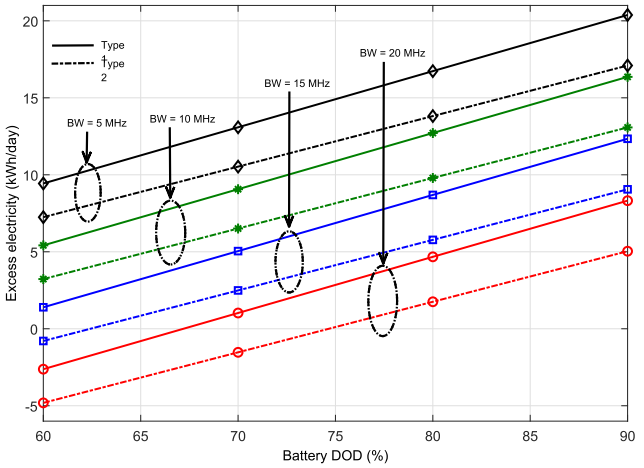

FIGURE 12. Excess electricity vs B_{DOD} varying $\mathcal{BW}$ for different battery types.

in the graph implies the zero fuel consumption (ZFC) state of different scenarios. For instance, the DG energy contribution will drop to zero if the C_{sol} are 4kW, 5kW, 6kW and 7kW for bandwidth of 5MHz, 10MHz, 15MHz and 20MHz respectively. In other words, the deployed standalone solar array can carry the BS load independently without any support from external retailers or DG supply under ZFC condition.

c: BATTERY BANK

Battery bank autonomy hours can be computed with the help of Eq. (25) for $\mathcal{BW} = 10$ MHz, $L_f = 0.2$ configuration; ($N_{bat} = 16 \times V_{nom} = 6\text{V} \times Q_{nom} = 360$ Ah $\times B_{DOD} = 0.7 \times 24$hr)/daily BS load, $L_{BS} = 16.47$ kWh. According to the calculation ESS can support the BS load for 35.25 hours independently during the absence of hybrid power supplies. Fig. 11 shows the battery autonomy (B_{aut}) with the variation of load factor for different bandwidth. A higher value of B_{aut} is preferable to handle BS load for a prolonged period of time. With the increment of bandwidth and load factor, B_{aut} curve moves downward which means higher load consumption that considerably reduced the battery bank charging time. However, B_{aut} shows superior performance for the lower $\mathcal{BW}$ and smaller load demand as illustrated from the figure. For example, ESS can support the BS load about 40 hours autonomously under 10 MHz bandwidth and 50% traffic intensity without any assistance from either green EH or DG module which is enough time for maintenance during malfunctions. It can be safely inferred that sufficient battery bank ensure a greater level of reliability without sacrificing QoS.

d: EXCESS ELECTRICITY

Fig. 12 depicts the daily surplus energy generation (E_{sur}) with battery depth of discharge (B_{DOD}) varying system bandwidth. The figure is also derived for the two commonly used storage devices for evaluating their impact on E_{sur}. According to the definition, B_{DOD} is a function of battery state of charge (B_{SOC}) and hence, the storage capacity directly depends on B_{SOC}. As a consequence, net energy production from the combined sources inherently moves upward direction with the higher value of B_{DOD}, this in turns resulting higher excess

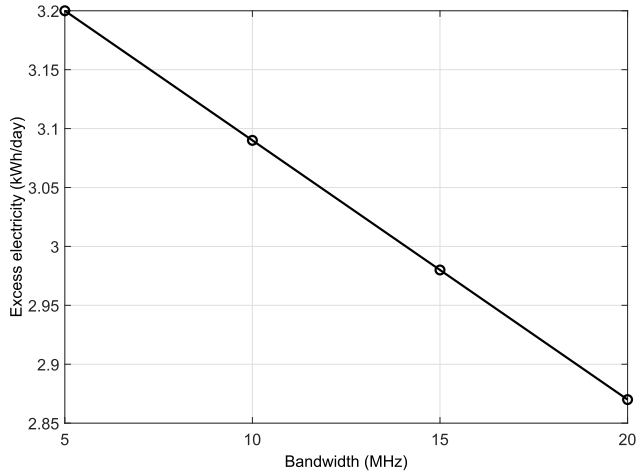

FIGURE 13. Excess electricity at zero fuel consumption.

electricity generation as evident from the figure. On the other hand, a large $\mathcal{BW}$ minimizes the E_{sur} due to greater load consumption as explained beforehand. In addition, ESS with higher nominal capacity exhibits optimistic performance compared to type-2 battery bank and therefore, type-1 lead-acid battery bank is considered over the entire manuscript.

Fig. 13 shows the daily surplus energy production under zero fuel consumption for various bandwidth. The curve is sharply falling down to reach the bottom point with the increment of $\mathcal{BW}$ as derived from the ZFC state of Fig. 10. Since ZFC condition is achieved for $C_{sol} = 7$kW panel capacity for 20 MHz bandwidth, while 4 kW solar PV array ensure no DG running hours under $\mathcal{BW} = 5$ MHz. Consequently, E_{sur} production is linearly scaled with C_{sol} and $\mathcal{BW}$ as well hence, larger solar panel capacity produce the bigger amount of E_{sur} even though the greater load consumption at higher bandwidth.

Fig. 14 demonstrates surplus electricity production for different bandwidth with the active number of resource blocks.

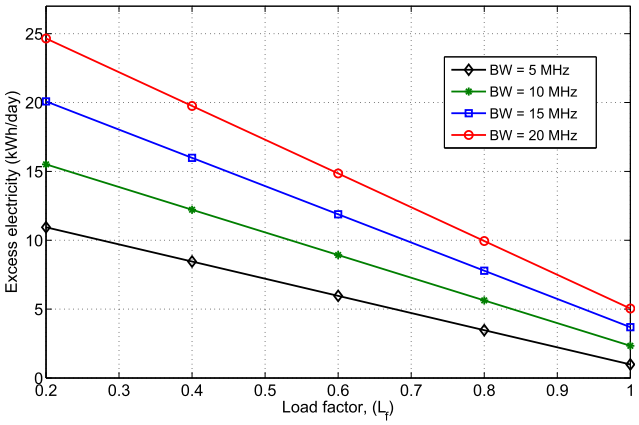

FIGURE 14. Excess electricity vs load factor (L_f) varying $\mathcal{BW}$.

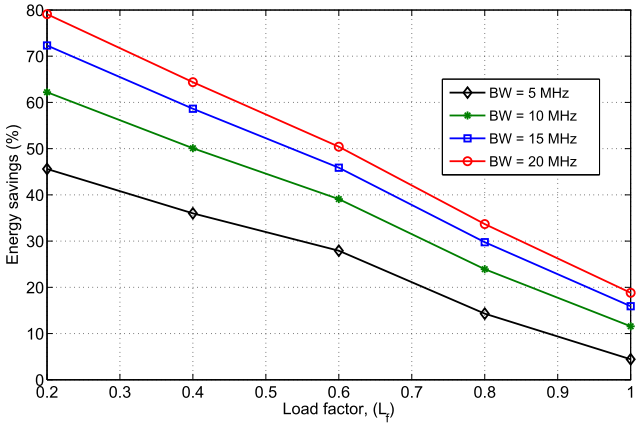

FIGURE 16. Energy savings percentage vs L_f for different $\mathcal{BW}$.

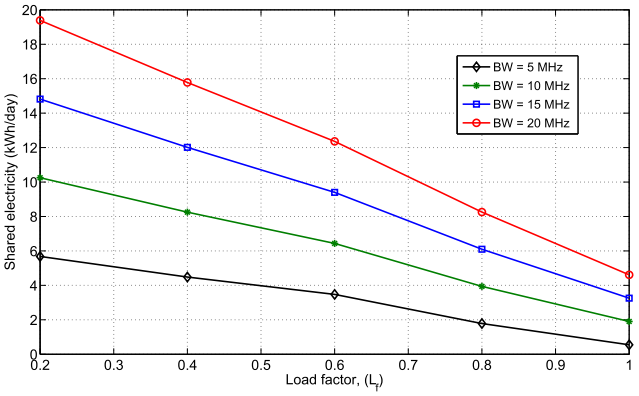

FIGURE 15. Shared electricity vs load factor for different $\mathcal{BW}$.

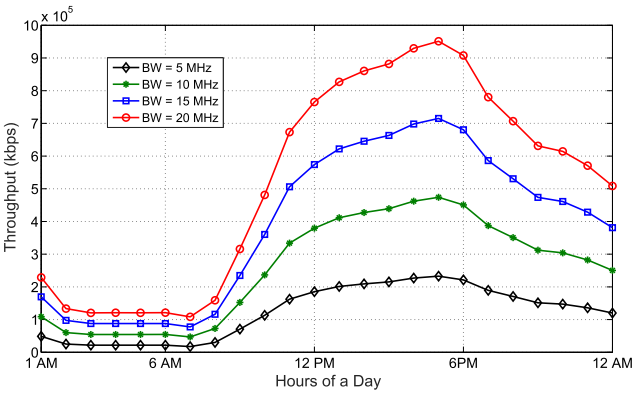

FIGURE 17. Throughput performance over a day for various $\mathcal{BW}$.

All the curves follows a similar pattern to reach their minimum values with the increment of L_f. Furthermore, the curve for larger $\mathcal{BW}$ outperforms than other ones because of its bigger EH installed capacity as evident from the graph. Notably, the figure is derived for the solar capacity at ZFC condition under all cases of load factor. As a result, a healthy amount of E_{sur} generated under low traffic intensity for all curves.

e: ENERGY SAVINGS

The mathematical model of energy savings via locally available green energy cooperation mechanism is clearly presented in section II-H. According to the definition, the sharable energy between surrounded BSs can be computed by subtracting transmission line loss from the surplus production. Fig. 15 describes the net amount of energy transferred to the closest neighboring BS for different load factor varying $\mathcal{BW}$. As expected, Fig. 15 follows a similar pattern of Fig. 14. Likewise, Fig. 16 manifest the percentage of energy savings for a single BS derived from the Fig. 15 based on Eq. (29). The maximum energy saving is attained at low L_f and higher $\mathcal{BW}$ which is about 80% and it gradually falls down with the increment of traffic demand. It can be concluded that the energy trading technique allows maximum utilization of solar energy and helps in further curtailing diesel consumption as well as emission intensive greenhouse gases.

3) ENERGY EFFICIENCY

Fig. 17 depicts the network throughput for distinct bandwidth considering inter-cell interference over 24 hours period. However, throughput is a function of resource block (RB) i.e. load factor. According to our assumption in the simulation setup section, the number of occupied RBs directly varied with a traffic profile. It is clearly evident from the figure that all the curves apparently follows the given traffic pattern presented in Fig. 3. Moreover, a noticeable throughput distribution gap is found between low arrivals and high traffic demands due to the variation of occupied RBs allocation. The traffic loading parameter $\chi = 0.8$ implies that 80% of RBs are occupied by the network. That is 40 RBs are occupied at a time while 10 RBs remains free to take further arrivals under the system operating with 10 MHz bandwidth. In accordance with Shanon's information capacity, throughput is proportionally related with received signal quality i.e. SINR which is a key parameter while measuring EE. Therefore, a UE receives the best signal quality under higher bandwidth as

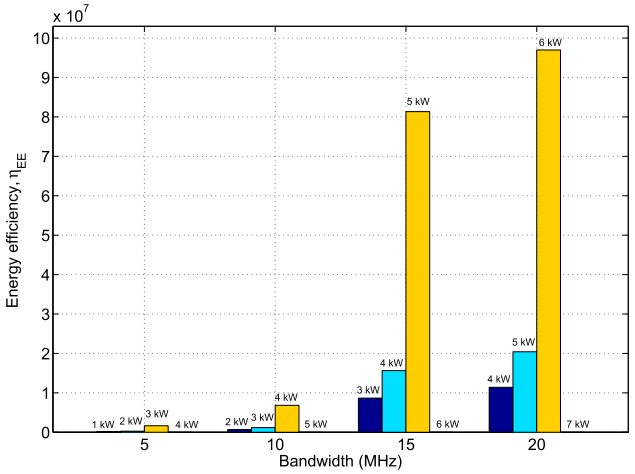

FIGURE 18. Energy efficiency vs $\mathcal{BW}$ for different PV capacity.

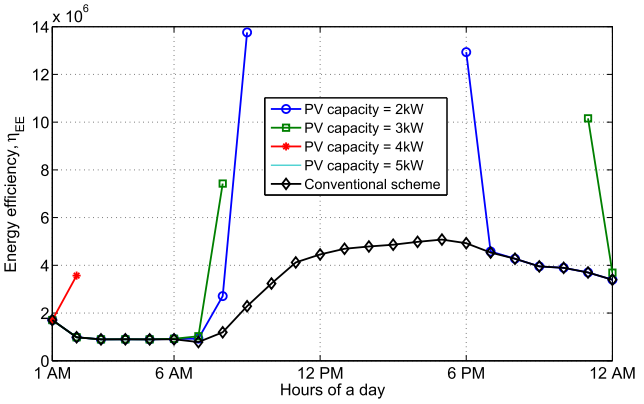

FIGURE 19. EE for $BW = 10$MHz varying PV capacity.

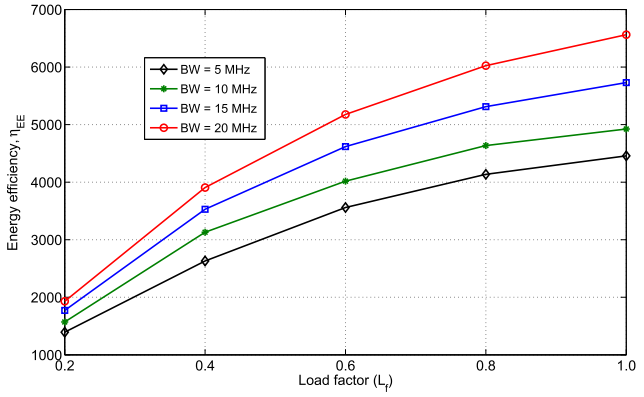

FIGURE 20. Energy efficiency vs L_f varying $\mathcal{BW}$.

observed from the figure. On the other hand, JT CoMP technique provides the best throughput performance owing to its joint coordination and thus uplifts spectral efficiency as well as EE performance for the considered hybrid scheme.

A quantitative comparison of EE performance with the system bandwidth is demonstrated in Fig. 18 which is obtained using Fig. 9 and Fig. 10 based on Eq. (36). The PV energy contribution and E_{DG} production follow an opposite trend to fulfill BS demand for various solar capacity as clearly noticed from Fig. 9 and Fig. 10. According to the definition, EE is inversely related to diesel energy contribution. Besides, higher PV array significantly reduces fuel consumption and thereby improves the EE performance as evident from Fig. 19. The empty region in the fourth column denotes the ZFC state for the four different cases where EE values become infinite because of zero E_{DG}. However, a profound impact of C_{sol} has been observed on EE performance as it moves upward direction rapidly with the increment of C_{sol}. In addition, EE is found less significant in the first two cases compared to the third column where the green energy support is dominating under all scenarios. Finally, it can be inferred that a higher EH capacity improves the EE performances with minimum environmental pollution.

For a better understanding of Fig. 18, a clear distinction of EE performance throughout the day varying C_{sol} for $\mathcal{BW} = 10$ MHz is illustrated in Fig. 19. The graph also includes EE curve for the conventional scheme in where the BS is running only diesel energy source. With the help of Fig. 5, EE curve goes upward direction rapidly with the increment of solar radiation intensity. For EH capacity of 2kW and 3kW, the EE goes to infinity after morning with the increment of solar PV power production and once again fall down sharply with the diminishing of sunlight. During midnight EE goes lower due to unavailability of sunlight and shortage of storage capacity and thus consume energy from DG supply to run the BS. The infinity EE region is identified by drawing no line in the figure denotes power consumption from DG goes to zero. During this period, the BS is fully run by solar energy in assistance with a battery bank. However, the empty horizon is more apparent for higher PV installed capacity implying that EH could carry BS demand for a prolonged period of time. All the curves of 2kW, 3kW and 4kW distribution follows identical behavior except the conventional one which exhibits the pessimistic performance. However, BS operating of 4 kW solar shows outstanding EE performance compared to other systems as it takes the lowest amount of fuel and serve the BS load almost all over 24 hours duration. Under this condition, the storage capacity is sufficient enough to feed BS load without any energy taken from DG supply during the absence of PV sources as observed from the figure. On the other hand, $C_{sol} = 5$kW indicates the zero fuel consumption condition in where EE has become infinity for the whole day because of that no curve is plotted on the figure.

Energy efficiency versus load factor varying bandwidth is presented in Fig. 20. The number of PV modules linearly scaled with L_f by reducing DG energy contribution as explained beforehand. Based on this information, all the curves in Fig. 20 follows homogeneous style to reach their maximum value with the load factor. EE performance for $\mathcal{BW} = 20$MHz perform a lot better than other curves presented in the figure. This is due to the fact that increased throughput and lower diesel consumption forces EE metric to rise.

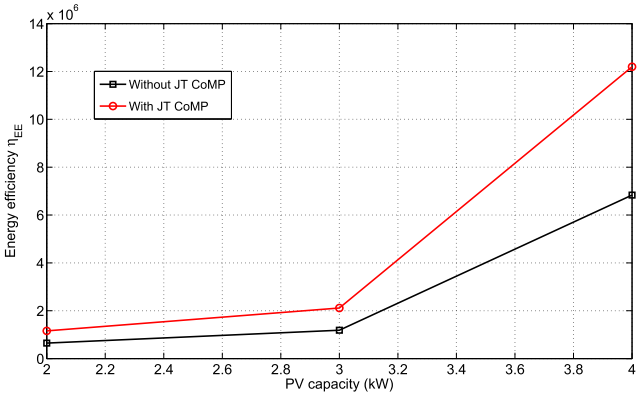

FIGURE 21. Energy efficiency vs PV capacity for $\mathcal{BW} = 10$MHz.

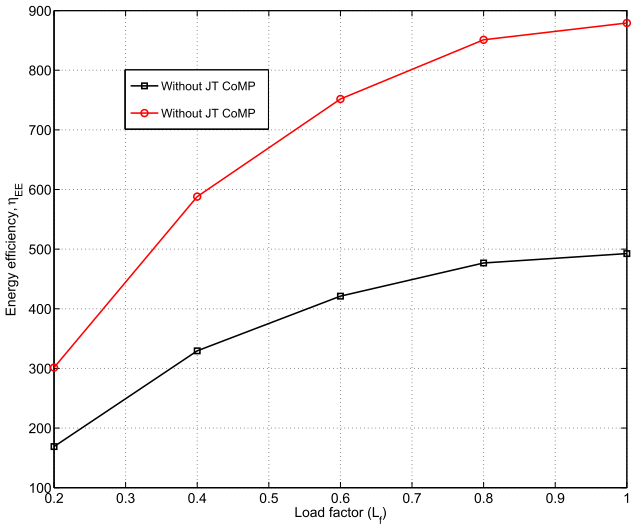

FIGURE 22. EE for $\mathcal{BW} = 10$MHz varying load factor.

A comparison of EE between the hybrid system without JT CoMP and with coordination for the given PV array capacity under 10 MHz bandwidth is demonstrated in Fig. 21. JT CoMP enabled proposed hybrid scheme indicates improved EE performance over non-CoMP based hybrid system because of better throughput performance. Moreover, EE gap is more apparent under higher green EH capacity where the variation of E_{DG} is also significant. Fig. 22 compares the EE metric variation of the proposed framework with the existing hybrid system without coordination mechanism for different load factor under particular network settings. Once again the proposed JT CoMP based hybrid power supply system achieves superior performance which is more remarkable for higher values of L_f.

Fig. 23 presents the energy efficiency index (EEI) comparison with the system bandwidth. The proposed system attains about 43.8% and 48.7% more energy efficient over non-CoMP hybrid system for $\mathcal{BW} = 10$MHz and 20 MHz respectively. It can be safely inferred that a RRH enabled LTE-A cellular networks with joint coordination is more preferable than conventional hybrid scheme.

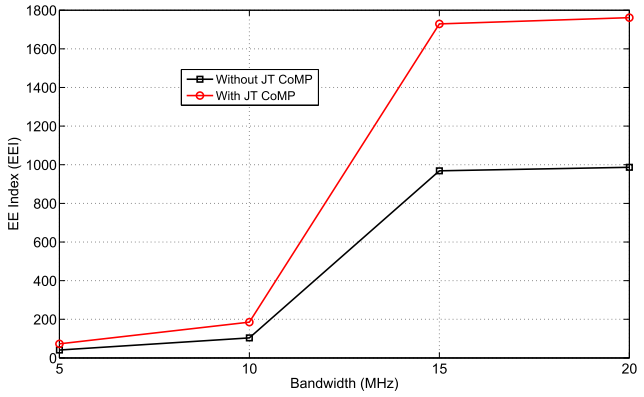

FIGURE 23. Comparison of energy efficiency index.

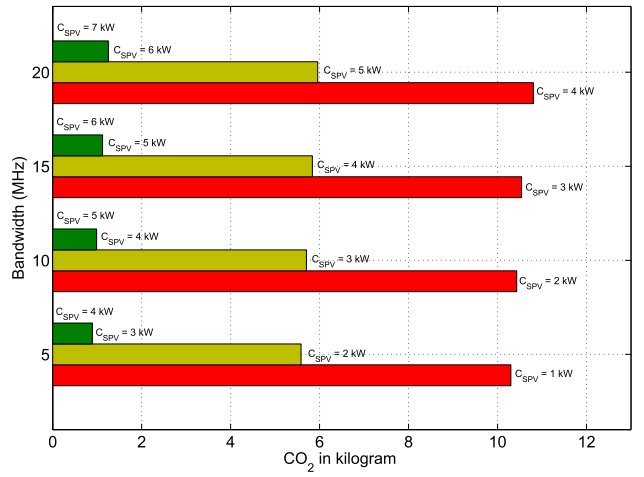

FIGURE 24. CO_2 emissions for various PV capacity and $\mathcal{BW}$.

4) GREENHOUSE GAS (GHG) EMISSIONS

A quantitative comparison of carbon dioxide ejections for different PV capacity and $\mathcal{BW}$ is illustrated in Fig. 24. In general, a DG set emit 2.68 CO_2 kg per liter and consume fuel of 0.39 L/kWh [38]. This graph reflected the pessimistic image of harnessing DG energy. As expected, there is no carbon emission for zero fuel consumption as depicted from the figure. Additionally, carbon footprint is found lower for higher PV capacity as explained using Fig. 10. For instance, the carbon emission is around 10 kilograms for PV capacity of 2 kW and reduced to zero when C_{sol} is 5 kW as no DG power is required under $\mathcal{BW} = 10$MHz. In summary, SPV/DG hybrid scheme with JT CoMP has been proved as an energy-efficient and feasible solution through enhancing EE performance for the envisioned off-grid green cellular networks especially in remote areas.

IV. CONCLUSIONS

This paper has examined the energy efficiency performances with a hybrid powered off-grid LTE-A macrocell BS endeavoring maximum usage of renewable energy. In light of this, an energy cooperation strategy based on surplus electricity

has been investigated for the envisaged green cellular networks. Joint transmission CoMP technique is also integrated with the contemplated framework for further improvement of EE. System performances in terms of sizing of installed power supply capacity, battery bank autonomy hours, aggregate energy contribution, surplus electricity, throughput, EEI, and energy savings have been thoroughly analyzed varying different parameters. The battery bank carried out the BS load independently for a prolonged period of time during hybrid supply malfunctioning. Results demonstrate that dual axis tracking mode PV array with high nominal battery bank capacity shows superior system performance compared to others. A significant impact of system bandwidth and load factor is noticed on CoMP and non-CoMP based networks. Moreover, a remarkable EE performance is observed with the increment of load factor owing to higher resource allocation and higher SPV capacity. Meanwhile, a solar energy sharing paradigm considerably increased EE further curtailing diesel consumption with lower greenhouse gas emissions. To the end, the level of EE performance substantially relies on a range of network setups. Future extension of this work will focus on green aware user association developing generalized algorithms and analytical modeling for heterogeneous networks with the verification by the simulation results.

REFERENCES

[1] Cisco, "Cisco visual networking index: Global mobile data traffic forecast update, 2016–2021," Cisco, San Jose, CA, USA, White Paper C11-738429, Feb. 2017.

[2] T. Kim and J. M. Chang, "QoS-aware energy-efficient association and resource scheduling for HetNets," *IEEE Trans. Veh. Technol.*, vol. 67, no. 1, pp. 650–664, Jan. 2018.

[3] K. Kanwal, G. A. Safdar, M. Ur-Rehman, and X. Yang, "Energy management in LTE networks," *IEEE Access*, vol. 5, no. 1, pp. 4264–4284, Mar. 2018.

[4] M. A. Marsan, G. Bucalo, A. Di Caro, M. Meo, and Y. Zhang, "Towards zero grid electricity networking: Powering BSs with renewable energy sources," in *Proc. IEEE Int. Conf. Commun. Workshops (ICC)*, Budapest, Hungary, Jun. 2013, pp. 596–601.

[5] A. Jahid and S. Hossain, "Dimensioning of zero grid electricity cellular networking with solar powered off-grid BS," in *Proc. IEEE Int. Conf. Elect. Electron. Eng. (ICEEE)*, Rajshahi, Bangladesh, Dec. 2017, pp. 1–4.

[6] A. Jahid, A. S. Ahmad, and M. F. Hossain, "Energy efficient BS cooperation in DPS CoMP based cellular networks with hybrid power supply," in *Proc. IEEE Int. Conf. Comput. Inf. Technol. (ICCIT)*, Dhaka, Bangladesh, Dec. 2016, pp. 93–98.

[7] M. Ismail, W. Zhuang, E. Serpedin, and K. Qaraqe, "A survey on green mobile networking: From the perspectives of network operators and mobile users," *IEEE Commun. Surveys Tuts.*, vol. 17, no. 3, pp. 1535–1556, 3rd Quart., 2014.

[8] A. Jahid, M. K. H. Monju, M. E. Hossain, and M. F. Hossain, "Renewable energy assisted cost aware sustainable off-grid base stations with energy cooperation," *IEEE Access*, vol. 6, pp. 60900–60920, Oct. 2018.

[9] M. A. Safwat, "Framework for multi-operator collaboration for green communication," *IEEE Access*, vol. 6, pp. 850–865, Nov. 2018.

[10] A. S. Aziz, M. F. N. Tajuddin, M. R. Adzman, and M. A. M. Ramli, "Feasibility analysis of PV/diesel/battery hybrid energy system using multi-year module," *Int. J. Renew. Energy Res.*, vol. 8, no. 4, pp. 1980–1993, Dec. 2018.

[11] A. Abrol and R. K. Jha, "Power optimization in 5G networks: A step towards GrEEn communication," *IEEE Access*, vol. 4, pp. 1355–1374, 2016.

[12] P. Gandotra, R. K. Jha, and S. Jain, "Green communication in next generation cellular networks: A survey," *IEEE Access*, vol. 5, pp. 11727–11758, 2017.

[13] H. Ghazzai, E. Yaacoub, A. Kadri, H. Yanikomeroglu, and M.-S. Alouini, "Next-generation environment-aware cellular networks: Modern green techniques and implementation challenges," *IEEE Access*, vol. 4, no. 1, pp. 5010–5029, Sep. 2016.

[14] M. S. Hossain, A. Jahid, and M. F. Rahman, "Quantifying potential of hybrid PV/WT power supplies for off-grid LTE base station," in *Proc. IEEE Int. Conf. Comput., Commun., Chem., Mater. Electron. Eng. (IC4ME2)*, Rajshahi, Bangladesh, Feb. 2018, pp. 1–5.

[15] D. Renga and M. Meo, "Dimensioning renewable energy systems to power mobile networks," *IEEE Trans. Green Commun. Netw.*, vol. 3, no. 2, pp. 366–380, Jan. 2019.

[16] A. Jahid, A. B. Shams, and M. F. Hossain, "Dynamic point selection CoMP enabled hybrid powered green cellular networks," *Comput. Elect. Eng.*, vol. 72, no. 1, pp. 1006–1020, Nov. 2018.

[17] P.-H. Chiang, R. B. Guruprasad, and S. Dey, "Optimal use of harvested solar, hybrid storage and base station resources for green cellular networks," *IEEE Trans. Green Commun. Netw.*, vol. 2, no. 3, pp. 707–720, Sep. 2018.

[18] A. Jahid, A. B. Shams, and M. F. Hossain, "Energy efficiency of JT CoMP based green powered LTE-A cellular networks," in *Proc. IEEE Int. Conf. Wireless Commun., Signal Process. Netw. (WiSPNET)*, Chennai, India, Mar. 2017, pp. 1739–1745.

[19] J. Leithon, T. J. Lim, and S. Sun, "Cost-aware renewable energy management with application in cellular networks," *IEEE Trans. Green Commun. Netw.*, vol. 2, no. 1, pp. 316–326, Mar. 2018.

[20] A. Jahid and M. S. Hossain, "Energy-cost aware hybrid power system for off-grid base stations under green cellular networks," in *Proc. 3rd IEEE Int. Conf. Electr. Inf. Commun. Technol. (EICT)*, Khulna, Bangladesh, Dec. 2017, pp. 1–6.

[21] M. H. Alsharif, R. Nordin, and M. Ismail, "Energy optimisation of hybrid off-grid system for remote telecommunication base station deployment in Malaysia," *EURASIP J. Wireless Commun. Netw.*, vol. 2015, no. 1, p. 64, Dec. 2015.

[22] T. Han and N. Ansari, "On optimizing green energy utilization for cellular networks with hybrid energy supplies," *IEEE Trans. Wireless Commun.*, vol. 12, no. 8, pp. 3872–3882, Aug. 2013.

[23] B. Wang, Q. Kong, W. Liu, and L. T. Yang, "On efficient utilization of green energy in heterogeneous cellular networks," *IEEE Syst. J.*, vol. 11, no. 2, pp. 846–857, Jun. 2017.

[24] M. H. Alsharif and J. Kim, "Hybrid off-grid SPV/WTG power system for remote cellular base stations towards green and sustainable cellular networks in South Korea," *Energies*, vol. 10, no. 1, p. 9, Dec. 2016.

[25] L. A. Fletscher, L. A. Suárez, D. Grace, C. V. Peroni, and J. M. Maestre, "Energy-aware resource management in heterogeneous cellular networks with hybrid energy sources," *IEEE Trans. Netw. Service Manage.*, vol. 16, no. 1, pp. 279–293, Mar. 2019.

[26] D. Benda, X. Chu, S. Sun, T. Q. S. Quek, and A. Buckley, "Renewable energy sharing among base stations as a min-cost-max-flow optimization problem," *IEEE Trans. Green Commun. Netw.*, vol. 3, no. 1, pp. 67–78, Mar. 2019.

[27] A. Jahid and M. S. Hossain, "Intelligent energy cooperation framework for green cellular base stations," in *Proc. IEEE Int. Conf. Comput., Commun., Chem., Mater. Electron. Eng. (IC4ME2)*, Rajshahi, Bangladesh, Feb. 2018, pp. 524–529.

[28] M. J. Farooq, H. Ghazzai, A. Kadri, H. ElSawy, and M.-S. Alouini, "A hybrid energy sharing framework for green cellular networks," *IEEE Trans. Commun.*, vol. 65, no. 2, pp. 918–934, Feb. 2017.

[29] F. Ahmed, M. Naeem, W. Ejaz, M. Iqbal, A. Anpalagan, and H. S. Kim, "Renewable energy assisted traffic aware cellular base station energy cooperation," *Energies*, vol. 11, no. 1, p. 99, Dec. 2018.

[30] Y.-K. Chia, S. Sun, and R. Zhang, "Energy cooperation in cellular networks with renewable powered base stations," *IEEE Trans. Wireless Commun.*, vol. 13, no. 12, pp. 6996–7010, Dec. 2014.

[31] B. Xu, Y. Chen, J. R. Carrión, J. Loo, and A. Vinal, "Energy-aware power control in energy cooperation aided millimeter wave cellular networks with renewable energy resources," *IEEE Access*, vol. 5, pp. 432–442, 2017.

[32] H. Ghazzai and A. Kadri, "Joint demand-side management in smart grid for green collaborative mobile operators under dynamic pricing and fairness setup," *IEEE Trans. Green Commun. Netw.*, vol. 1, no. 1, pp. 74–88, Mar. 2017.

[33] Y. Wu, V. K. N. Lau, D. H. K. Tsang, L. P. Qian, and L. Meng, "Optimal energy scheduling for residential smart grid with centralized renewable energy source," *IEEE Syst. J.*, vol. 8, no. 2, pp. 562–576, Jun. 2014.
[34] S. Zhang, N. Zhang, S. Zhou, J. Gong, Z. Niu, and X. Shen, "Energy-aware traffic offloading for green heterogeneous networks," *IEEE J. Sel. Areas Commun.*, vol. 34, no. 5, pp. 1116–1129, May 2016.
[35] A. Hajisami and D. Pompili, "Dynamic joint processing: Achieving high spectral efficiency in uplink 5G cellular networks," *Comput. Netw.*, vol. 126, pp. 44–56, Jun. 2017.
[36] A. Jahid, A. B. Shams, and M. F. Hossain, "Green energy driven cellular networks with JT CoMP technique," *Phys. Commun.*, vol. 28, pp. 58–68, Jun. 2018.
[37] F. Qamar, K. B. Dimyati, M. N. Hindia, K. A. B. Noordin, and A. M. Al-Samman, "A comprehensive review on coordinated multi-point operation for LTE-A," *Comput. Netw.*, vol. 123, pp. 19–37, Aug. 2017.
[38] A. Jahid, M. H. Monju, M. S. Hossain, and M. F. Hossain, "Hybrid power supply solutions for off-grid green wireless networks," *Int. J. Green Energy*, vol. 16, no. 1, pp. 12–33, Oct. 2018.
[39] Solaris Technology Industry. *American Conductor Wire Size*. Accessed: Feb. 27, 2019. [Online]. Available: https://www.solarisshop.com/content/AmericanWireGaugeConductorSizeTable.pdf

ABU JAHID (S'17) received the bachelor's and M.Sc. degrees in electrical engineering from Military Institute of Science and Technology (MIST), Dhaka, Bangladesh. From 2010 to 2012, he worked as a BSS Engineer with the Huawei Technologies, where he researches on radio network planning and optimization. Since 2016, he has been serving as an Assistant Professor with the Department of EEE, Bangladesh University of Business and Technology, Dhaka, Bangladesh. He has coauthored numerous articles in prestigious journals and IEEE conference proceedings. His research interests include modeling of energy efficient green cellular networks. He has been serving as TPC member, and Reviewer for many reputed international journals and conferences.

MD. SHAMIMUL ISLAM received the B.Sc. degrees in electrical and electronic engineering (EEE) from the University of Information Technology and Sciences (UITS), Dhaka, Bangladesh, in 2013. From 2015 to 2016, he worked as a Lab Demonstrator with the Department of Electrical and Electronic Engineering, UITS. Since 2016, he has been working as a Lab Assistant with the Department of Electrical and Electronic Engineering, Bangladesh University of Business and Technology (BUBT). His research interests include the design cellular communications and renewable energy system.

MD. SANWAR HOSSAIN received the B.Sc. degrees in electrical and electronic engineering (EEE) from the Rajshahi University of Engineering and Technology, Rajshahi, Bangladesh, in 2010. He is currently pursuing the M.Sc. degree in electrical electronic and communication engineering with the Military Institute of Science and Technology (MIST). From 2011 to 2015, he was a Lecturer and currently he has been serving as an Assistant Professor with the Department of EEE, Bangladesh University of Business and Technology, Dhaka, Bangladesh. His research interests include green energy, smart grid, and power system optimization.

MD. EMRAN HOSSAIN received the bachelor's degree in electrical and electronic engineering from Bangladesh University of Business and Technology (BUBT), in 2018. His current research interests include green communications and optimization.

MD. KAMRUL HASAN MONJU received the B.Sc. degree in electrical engineering from Bangladesh University of Business and Technology (BUBT), Dhaka, Bangladesh, in 2018. His current research interests include wireless communications and renewable energy.

MD. FARHAD HOSSAIN (S'10-M'14) received the B.Sc. and M.Sc. degrees in electrical and electronic engineering (EEE) from Bangladesh University of Engineering and Technology (BUET), Dhaka, Bangladesh in 2003 and 2005, respectively, and the Ph.D. degree in electrical and information engineering from the University of Sydney, Australia, in 2014. Currently, he holds a position of Professor with the Department of EEE. He also works as an electrical and electronic engineering Consultant. He has published over 50 refereed articles in highly prestigious journals and conference proceedings. He was the recipient of Best Paper Award in three international conferences and the Student Travel Grant in IEEE Global Communications Conference (GLOBECOM), Anaheim, CA, USA, 2012. His research interests include green cellular networks, underwater communications, smart grid communications, sensor networks, network architectures, and protocols designs, etc. He has been serving as TPC member, and Reviewer for many international journals and conferences.